Numerical analysis of real fluid behavior effects on a sliding-vane compressor comprehensive model

Stefano Gianoncelli[1], Andrea Genoni[1], Ida Costanzo[2], Stefano Murgia[2], Abdullah Bamoshmoosh[1], Gianluca Valenti[1, *, [0000-0003-4161-903X]]

[1] Department of Energy, Politecnico di Milano, Via Lambruschini 4/A, 20156 Milano, Italy;
[2] Ing. Enea Mattei S.p.A, Strada Padana Superiore 307, Vimodrone, 20055 Milano, Italy;
[*]Correspondence: gianluca.valenti@polimi.it

Abstract. This work presents a simulation model on a sliding vane compressor based on a lumped parameter model. The model is capable of predicting the performance of sliding-vane compressors. The model is divided into different subsections to evaluate the compressor's geometry, kinetics, thermodynamics, and rotor dynamics. The output of the tool includes the compressor unit's performance, such as volumetric flow rate, mechanical power, and process efficiency. The study examines the tool's ability to perform quick and efficient analyses using using either ideal or real fluid characterization, based on the REFPROP code. The code is validated against one experimental point. Simulations were conducted on a mid-size sliding-vane rotary compressor operating with three different types of working fluids from 20 °C and 1 bar (absolute) to 11 bar at 1500 rpm. In the ideal fluid case, simulations took 10-27 seconds, while real fluid assumptions took 1,038-4,329 seconds. The volumetric flow rate was influenced by the gas used, but changes among fluid models were not substantial, with a mean absolute percent difference of 0.5%. Mechanical power consumption was affected by the fluid choice and gas model, leading to a mechanical power difference between 0.4% and 1.1% in the ideal gas case. The specific mechanical work showed greater deviations among the fluids, with methane molar mass coherently increasing its value. Results show that the model developed is able to assess the major phenomena of sliding-vane compressors, and the ideal fluid model should be preferred when possible since computational times are significantly reduced with comparable results.

Keywords: Sliding-vane compressor; numerical simulation; compressor performance; fluid model.

1 Introduction

The consumption of compressed air in the industrial, commercial, and residential sectors accounts for a significant percentage of electrical energy usage, ranging from 6% to 20% [1]. As a result, manufacturers in these sectors must prioritize energy efficiency and reliability to ensure a sustainable and affordable future for end-users. Given that the rotary compressors play a significant role in the compressed air market,

this article focuses on the development of a comprehensive model for simulating the primary phenomena of sliding-vane compressors to enhance their performance. The computer model has been developed over several years with a continuous effort to improve its completeness, accuracy, and robustness. The article examines its ability to perform quick and efficient analysis with both ideal and real fluid models by presenting and comparing the results of case studies that simulate three sliding-vane compressors using different types of working fluid, namely, air, methane, and a methane-carbon dioxide mixture.

The article starts by describing the numerical tool's structure, followed by an explanation of the implementation of the ideal and real fluid models. Then, the simulated compressor geometry, working conditions, and working fluids are presented to provide a comprehensive characterization of the experimental and numerical analysis. The results are subsequently presented, highlighting the most interesting outcomes of the simulations, followed by a summary of schematic and direct conclusions.

2 Comprehensive Model

The SVEC (Sliding Vane Efficient Compressor) software has been developed using MATLAB environment to simulate sliding-vane compressors and expanders. The software follows a multidisciplinary approach and is based on a comprehensive model divided into different sub-sections for theoretical and numerical analysis. The overall flow diagram is illustrated in Fig. 1, which is described in the next sections.

2.1 Input modules

Input structure includes two modules. The first module is CALL_SVEC, which is the user interface for inputting data either manually or by retrieving them from pre-compiled databases. The input parameters required by the software include machine geometry, thermodynamic boundaries of the process, and working fluid and lubricant properties. The input interface is divided into different sections, and the input data is packed into structures based on the information they contain. Additionally, the user can activate or deactivate additional controls and define simulation boundaries in a dedicated section, such as deciding whether to include inlet and outlet line components in the simulation. The input parameters are then converted into SI units and packed in the SVECpreProc module.

2.2 Main model

The core of the numerical model is included in SVECmodelMain. This module contains all the code subsections described below building a tiered execution structure.

S1-INPUT CHECK & UNPACKING
This module unpacks the input data previously gathered, loading them in the simulation workspace. All the data are checked for both logical and numerical consistency.

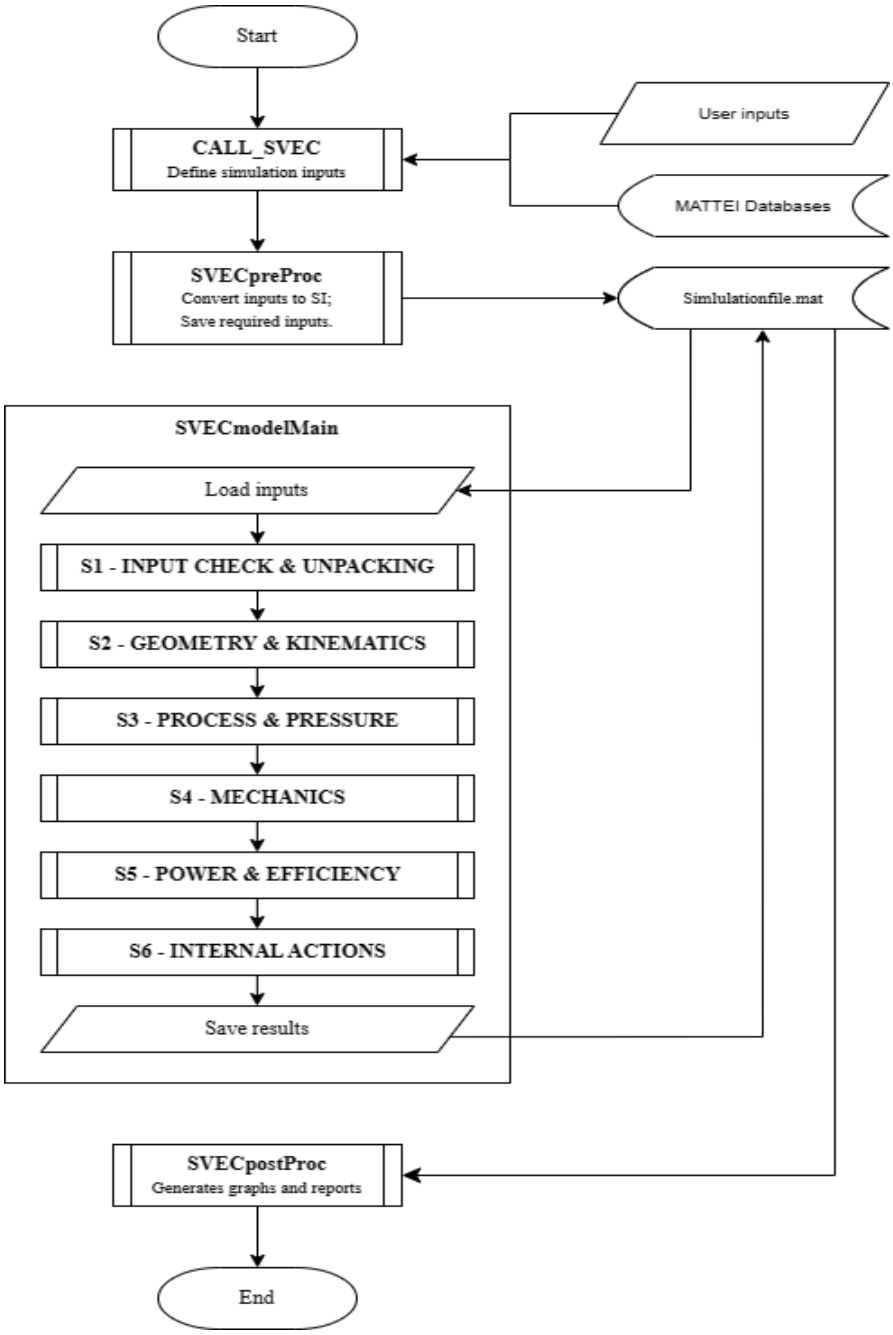

Fig. 1. Flow diagram of SVEC, the simulation tool for sliding-vane compressors performances evaluation. Each block in the diagram represents one of the internal functions of the software and is dual to a part of the theoretical comprehensive model characterising the compression process

S2-GEOMETRY AND KINEMATICS

This section performs an angular and temporal discretization of the process allowing to simulate the vane, stator and rotor motion in each angle and to compute velocities. Referring to Fig. 2, the vane center of gravity (F) position against time is computed via vector kinematic equations in exponential form and results are extended for symmetry to all vanes. Angle θ describes the vane kinematics relying on two reference systems: the inertial one along the vane axis and the absolute one fixed in the rotor center. Vane tip angles are defined according to [2], R is the stator radius, while r the rotor one.

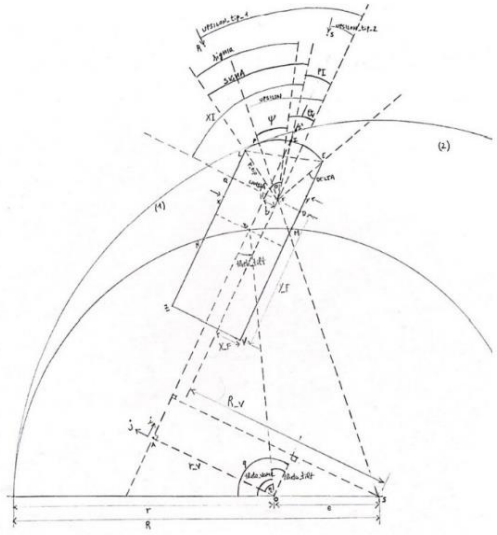

Fig. 2. Representation of the main geometrical quantities used for kinematic quantities evaluation. The inertial reference system is placed in point Z while the absolute one is in point O.

S3-PROCESS AND PRESSURE

This is the core of the thermodynamic model evaluating the working fluid temperature and pressure evolution according to section 2.3. Due to the computational complexity, different submodules are defined to cooperate with the main one, CHAMBER, able to compute the cell thermodynamic quantities in each point of a full revolution. Their purposes are to evaluate the oil injection inside the compression chamber and to compute the exploited mass flow rate and volumetric efficiency including leakages through main clearances. The effects of the suction and discharge processes outside the chamber are then included as well. Energy and mass balances are solved according to the fluid model selected, which can use ideal gas laws or real gas solution through the integration of REFPROP.

S4-MECHANICS

S4 oversees dynamic quantities evaluation. Once the pressure evolution inside the chamber is known, and the geometry, forces magnitude can be computed also including inertial effects [3]. The module is based on an adaptation of Huang *et al*. [4].

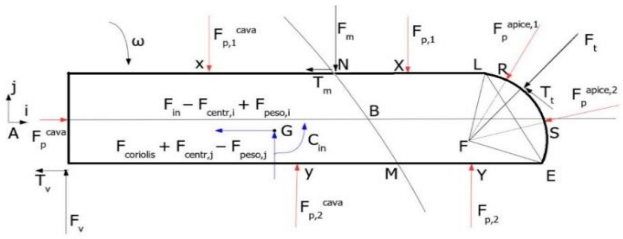

Fig. 3. Graphical representation of the forces acting on a vane. Pressure forces are labeled with *p*, friction ones with *t*.

Referring to Fig. 3, forces are reported to the absolute reference system through the transfer equations below. Firstly, resulting forces on a rotating reference system placed on vane axis are computed both in the perpendicular direction ($R_{\theta x}$) and on the tangential one ($R_{\theta y}$) starting from forces on the inertial reference system (i, j):

$$R_{\theta x} = \left(-F_m + F_v - F_{p1}^{slot} + F_{p2}^{slot}\right)\cos\theta_{tilt} + \left(T_m + T_v - F_p^{slot}\right)sin\theta_{tilt} \quad (1)$$

$$R_{\theta y} = -\left(-F_m + F_v - F_{p1}^{slot} + F_{p2}^{slot}\right)\sin\theta_{tilt} + \left(T_m + T_v - F_p^{slot}\right)cos\theta_{tilt} \quad (2)$$

where θ_{tilt} is the vane tilt angle with respect to radial direction while forces definition can be found in the related bibliography [4]. Equations 3 and 4 allow to compute the absolute horizontal (R_x) and vertical (R_y) forces resultant on the fixed reference system placed on rotor center i.e., point O in Fig. 2:

$$R_x = R_{\theta x}sin\theta_{vane} - R_{\theta y}cos\theta_{vane} \quad (3)$$

$$R_y = R_{\theta x}cos\theta_{vane} + R_{\theta y}sin\theta_{vane} \quad (4)$$

where θ_{vane} is the vane center of gravity angular position with respect to the horizontal.

S5-POWER & EFFICIENCY

Once the forces magnitude and their application points are known, the expected power consumption is computed. The shaft torque due to a single vane C_{vane} is computed via:

$$C_{vane} = F_m AM_i - F_v AV_i - sgnT_m\left(r_v + sgns_1\frac{s}{2}\right) - sgnT_v\left(r_v - sgns_2\frac{s}{2}\right) + F_{p1}^{slot}A_{x_i} - F_{p2}^{slot}A_{y_i} + sgnF_p^{slot}r_v \quad (5)$$

where subscript i points to a projection on the corresponding axis while sgn is a service coefficient allowing to extend the approach also for inclined vanes. In the right-hand side of the equation forces and their arms can be found, according to Fig. 3 and related bibliography. The overall resistant torque on the rotor, C_{tot}, is given by this contribution multiplied by the actual number of vanes and, finally, the overall power consumption P_{mecc} is computed through the mean integral of $C_{tot} * \omega$ over an entire revolution.

S6-INTERNAL ACTIONS
This is an elective module where the 3D state of stress of the vane is evaluated, and the equivalent mono dimensional value is computed for material stress-strain analysis.

2.3 Fluid Models

In this section, the two different approaches used to simulate the behavior of the fluids are described. Both approaches have separated models for the calculation of thermodynamic and transport properties. The first approach is the ideal gas approach. In the ideal gas approach, the density of the fluid is calculated through the ideal gas law, while the specific heat is equal to the ideal gas specific heat. The ideal gas specific heat is calculated through a fourth-degree polynomial which is a function of temperature [5]. The model for transport properties is based on the rarified kinetic gas theory. The formulation used in this work is the one given by Chung *et al*. [6]. The thermodynamic and transport models can be coupled easily as the assumptions for rarified kinetic gas theory and the ideal gas assumption are relatively similar. The second approach relaxes the ideal gas assumption. The thermodynamic properties are calculated using real fluid equations of state. The employed equations of state are the one present in the REFPROP routine. The three equations of state are Helmholtz free energy equations of state [7, 8, 9]. Air is treated as a pseudo-pure fluid. A specific equation of state is used for pure methane, while the natural gas standard GERG2008 is used for the carbon dioxide-methane mixture. Transport properties for air are calculated through a corrected kinetic gas theory model [10], while transport properties for methane and carbon dioxide are fitted from experimental data [11,12]. The leakage model used for these simulations is based on Poiseuille-Couette flow theory [13], which depends on the gas-oil mixture viscosity, evaluated basing on Awad *et al*. [14].

3 Case studies

The software needs data on the machine geometry, working conditions and exploited fluids; therefore, these aspects are here presented in order to furnish the useful context before discussing the simulations results. Both the experimental and the numerical campaign used the same compressor type. Due to the inflammability of working fluids 2 and 3 from Table 2, these latter are only tested numerically for safety reasons.

3.1 Machine geometry

A mid-sized sliding-vane rotary compressor is considered, consisting in a cylindrical stator (D = 136 mm) hosting an eccentric rotor (d = 111 mm), tangent to the former inner wall defining a contact line. This line divides suction and delivery regions, where inlet and outlet ports are carved inside the cast-iron stator. The sliding-vanes are seven and positioned inside of radial slots. When the machine is operating, vanes slide out from their slots, making contact with the stator inner wall and forming a closed volume named cell. The cell capacity varies depending on the angle of rotation, determining

the pressure variation of the fluid. As schematized in Fig. 4, suction phase lasts from 30.3° to 162.4° while discharge one spans from 326.1° to 356.1°. Vanes are 38 mm long and 4.72 mm thick, with an optimized tip radius equal to 9.5 mm.

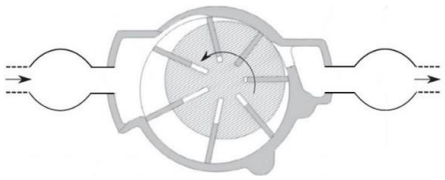

Fig. 4. Sliding vane compressor representation.

3.2 Numerical campaign

The numerical campaign assumed a standard rotational speed of 1500 rpm, while the working conditions and the exploited fluids are reported respectively in Table 1 and Table 2. Both the ideal and the real fluid models are tested.

Table 1. Simulation parameters (pressures are absolute).

Test	Inlet pressure [barA]	Outlet pressure [barA]	Inlet temperature [°C]
1, 2, 3	1	11	20

Table 2. Working fluid composition.

Test	Working fluid	Elements	Gas molar composition [%]	Molar mass [kg/kmol]	Dynamic viscosity [$\mu Pa\ s$]
1	Air	N_2, O_2, Ar, CO_2	78, 21, 0.93, 0.03	28.96	21.6
2	Methane	CH_4	100	16.04	13.2
3	Methane – CO_2	CH_4, CO_2	50, 50	30.03	13.5

3.3 Experimental validation

The experimental validation followed standards ISO 5167 and ISO 1217. The validation here presented is a test at 1500 rpm with air as working fluid with ambient conditions of 1 bar and 20 °C, with delivery pressure set at 7.5 barA.

Table 3. Results of the experimental campaign, compared with numerical results using ideal gas model. The percentage difference between the two values is reported in parenthesis.

Test	Volumetric flow rate [l/min]	Mechanical work [kW]	Specific mechanical work [kJ/kg]
Experimental	3,544.5 ± 0.7 %	24.3 ± 0.2 %	346.1 ± 0.8 %
Numerical	3,529.3 (-0.4%)	23.5 (-3.1%)	343.3 (-0.8%)

Table 3 compares the numerical data against the experimental ones: the three parameters proved the goodness of the comprehensive model, validating its implementation. The volumetric flow rate is the closest to the experimental data, with a percentage difference of 0.4%, proving the consistency of the cell volume evolution evaluation, the leakage models and the suction and discharge processes influence. Mechanical power is the less accurate with an error equal to 3.1% which is however considered acceptable.

4 Results and Discussion

This chapter presents and discusses the results of the numerical campaign. Common performance parameters of interest in compressors testing coming from the numerical campaign are presented in Table 4.

4.1 Numerical results

Simulations took 10 to 27 seconds in the ideal fluid case, 1,038 to 4,329 seconds with real fluid assumptions using REFPROP for properties evaluation on a 11th Gen Intel® Core i5-11600K @3.90GHz. The slowest test was number 1, due to the air molecular composition and complexity when compared to other gases. Basing on the process definition air, methane and CO2 can be in principle reasonably modelled as ideal fluids during the whole compression for every test.

Table 4. Results of the numerical campaign, obtained with both ideal and real gas modelling. The percentage difference between the two models is reported in parenthesis.

Test	Volumetric flow rate [l/min]		Mechanical power [kW]		Specific mechanical work (SMW) [kJ/kg]	
	ideal	real	ideal	real	ideal	real
1	3,513.1	3,508.2 (-0.1%)	27.35	27.23 (-0.4%)	393.2	391.9 (-0.3%)
2	3,290.6	3,273.1 (-0.5%)	25.85	25.70 (-0.6%)	716.1	714.4 (-0.2%)
3	3,465.4	3,490.6 (+0.7%)	25.83	25.56 (-1.1%)	363.1	355.5 (-2.1%)

Regarding the volumetric flow rate, the first and third test results are very similar (1.4% different) despite the fluid difference, which in general should not implicate a considerable disparity of performance since volumetric flow rate value is mainly influenced by the volume available in the first closed chamber and the rotational speed. The largest losses of volumetric efficiency are represented by the leakages between the three main clearances and to the fluid complexity. Differences in this value are mainly attributed to the rotor-stator leakage model selected. Despite Poiseuille-Couette is considered [15] to be the best overall performing model for sliding-vanes machinery, in this campaign it has shown to be quite sensible to the selected type of fluid, especially in scenarios where the viscosity and density of the fluid are particularly different from one another, leading to the result of test 2. Regarding the difference between the ideal and real gas thermodynamic model, volumetric flow rate changes among fluid models

are not substantial, with the mean absolute percent difference being 0.4%. A peculiar case is found in test number 3, where the real gas volumetric flow rate is higher than the ideal one. This is a consequence of the highly detailed heat exchange model in the real gas model, leading to an increased heat exchange between gas and oil and, consequently, a lower outlet gas temperature (27°C lower) and a higher and increased average viscosity due to the better molecules cohesion and, finally, a lower leaking flow rate in the real case scenario for this test.

The mechanical power results are greatly affected by the working fluid choice, with the highest difference being 6.1% between the air and the mixture cases with real fluid assumption. Even if the methane flow rate is generally the lowest, its specific heat capacity leads to a higher compressing work and thus the required power in the ideal case is more similar (0.1% higher) to the one necessary for the mixture compression than to the air one. In the case of mechanical power, the fluid model choice has an appreciable influence due to the impact of pressure evolution on forces and related power consumption and dissipation. In the meantime, adopting the real gas assumption instead of the ideal one shows deviations comparable to the ones encountered in the volumetric flow rate with the same assumptions, proving a good scaling effect between the two values. As a matter of fact, applying the real gas model led to a difference between 0.4% and 1.1% compared to the ideal gas case, similar to the 0.7% maximum difference encountered for the flow rate. Real gas scenario offers a mechanical power which is always lower than the one predicted in the ideal case, differently to the volumetric flow rate trend.

Lastly, the specific mechanical work (SMW) is directly related to the two previous parameters, being computed as the ratio between the mechanical power (P_{mech}) and the elaborated mass flow rate ($\dot{m}$). In the simple fluid scenario results show greater deviations among fluids, with the value of the second test being almost doubled with respect to the other two comparable results. In this case, differences are mainly due to the lower molar mass of the methane, causing a lower density and hence a lower mass flow rate that drastically increase the SMW. Comparing ideal and real fluid models, the maximum discrepancy is 7.6 kJ/kg absolute or 2.1% relative in the third test, due to the combined influence of the differences in volumetric flow rate and mechanical power.

5 Conclusions

In this work, a comprehensive model able to simulate sliding-vane compressors performances has been presented and experimentally validated, highlighting the implementation of both the models for ideal fluid and real fluid characterization.

- The model can properly assess main phenomena characterizing sliding-vane compressors and provide quick and accurate estimate of their performance parameters.
- Volumetric flow rate values are sensibly affected by the leakages path models. Fluid viscosity and molecular complexity have a considerable impact on results.
- Mechanical power consumption is both affected by the fluid choice and the gas model, being directly related to pressure evolution in the chamber and related forces.

- Ideal fluid model should be preferred when reasonable, depending on the process and fluid parameters since computational times are sensibly reduced with comparable results. When necessary, real fluid behavior can be assessed by choosing the proper equation of state model and using REFPROP for properties evaluation.

References

1. R. Cipollone. Sliding Vane Rotary Compressor Technology and Energy Saving. Proceedings of the Institution of Mechanical Engineers (230), 208–234 (2016).
2. C. Hong, L. Lianseng, G. Bei, S. Pengcheng. Research on tip profile of vane for rotary vane compressor. National Engineering Research Center for Fluid Machinery and Compressors, 2005.
3. X. Tojo, T. Kan, A. Arai. Dynamic Behavior of Sliding Vane in Small Rotary Compressors. International Compressor Engineering Conference, (1978).
4. Y. M. Huang, C. L. Li. Analysis of forces acting on compressor sliding vanes. Spring technical conference of the ASME internal combustion engine division, 2002.
5. B. E. Poling, J. M. Prausnitz and J.P. O'Connel, Properties of Gases and Liquids, 5th Edition, McGraw-Hill, 2001.
6. T.H Chung, L. L. Lee and K. E. Starling. Applications of Kinetic Gas Theories and Multiparameter Correlation for Prediction of Dilute Gas Viscosity and Thermal Conductivity, Ind. Eng. Chem. Fundam. 23, 8-13 (1984).
7. E. W. Lemmon, R. T. Jacobsen, S. G. Penoncello and D. G. Friend. Thermodynamic Properties of Air and Mixtures of Nitrogen, Argon and Oxygen From 60 to 2000 K at Pressures to 2000 MPa. Journal of Physical and Chemical Reference Data 29, 331 (2000).
8. U. Setzmann, W. Wagner. A New Equation of State and Tables of Thermodynamic Properties for Methane Covering the Range from the Melting Line to 625 K at Pressures up to 1000 MPa. Journal of Physical and Chemical Reference Data 20, 1061 (1991).
9. O. Kunz and W. Wagner. The GERG-2008 Wide-Range Equation of State for Natural Gases and Other Mixtures: An Expansion of GERG-2004. J. Chem. Eng. Data, 57, 11, 3032-3091 (2012).
10. E. W. Lemmon and R. T. Jacobsen. Viscosity and Thermal Conductivity Equations for Nitrogen, Oxygen, Argon and Air. International Journal of Thermophysics 25, 21-69 (2004).
11. B. A. Younglove and J. F. Ely. Thermophysical Properties of Fluids. II. Methane, Ethane, Propane, Isobutane, and Normal Butane. Journal of Physical and Chemical Reference Data 16, 577 (1987).
12. V. Vesovic and W. A. Wakeham. The Transport Properties of Carbon Dioxide. Journal of Physical and Chemical Reference Data 19, 763 (1990).
13. N. Nervegna, S. Mancò. Simulation of an External Gear Pump and Experimental Verification. Politecnico di Torino, (1987).
14. M. M. Awad, Y.S. Muzychka. Effective Property Models for Homogeneous Two-Phase Flows. Experimental Thermal and Fluid Science, (2008).
15. F. Fatigati, M. Di Bartolomeo, D. Di Battista and R. Cipollone. Experimental Validation of a New Modeling for the Design Optimization of a Sliding Vane Rotary Expander Operating in an ORC-Based Power Unit. Energies. 13 (2020).